Freeze–Thaw Resistance of Unidirectional-Fiber-Reinforced Epoxy Composites

Hui Li, Guijun Xian, Qi Lin, Hui Zhang

School of Civil Engineering, Harbin Institute of Technology, Harbin 150090, China

Received 26 October 2010; accepted 6 May 2011
DOI 10.1002/app.34870
Published online 28 September 2011 in Wiley Online Library (wileyonlinelibrary.com).

ABSTRACT: The freeze–thaw resistance of unidirectional glass-, carbon-, and basalt-fiber-reinforced polymer (GFRPs, CFRPs, and BFRPs, respectively) epoxy wet layups was investigated from −30 to 30°C in dry air. Embedded optic-fiber Bragg grating sensors were applied to monitor the variation of the internal strain during the freeze–thaw cycles, with which the coefficient of thermal expansion (CTE) was estimated. With the CTE values, the stresses developed in the matrix of the FRPs were calculated, and CFRPs were slightly higher than in the BFRP and GFRP cases. The freeze–thaw cycle showed a negligible effect on the tensile properties of both GFRP and BFRP but exhibited an adverse effect on CFRP, causing a reduction of 16% in the strength and 18% in the modulus after 90 freeze–thaw cycles. The susceptibility of the bonding between the carbon fibers and epoxy to the freeze–thaw cycles was assigned to the deterioration of CFRP. © 2011 Wiley Periodicals, Inc. J Appl Polym Sci 123: 3781–3788, 2012

Key words: ageing; composites; degradation

INTRODUCTION

In recent years, fiber-reinforced polymer (FRP) composites have been finding wide application in the upgrading and retrofitting of existing structures and the construction of new structures (e.g., FRP bridge decks) because of their obvious advantages, such as high strength, low density, and high corrosion resistance.[1,2] As an example, FRP wet layups or laminates are externally bonded to concrete structural (e.g., beam, slab, pier) surfaces to improve their loading capacity.[3,4] The durability of FRPs in harsh civil environments (e.g., water immersion, salt and alkaline solutions, high and low temperatures, freeze–thaw cycles) is one of the major concerns for civil engineering applications.[1] A number of investigations have been conducted on the durability of FRPs and FRP-related structures. Many positive experimental and practical results have already been reported.[5–7] Despite this, the lack of long-term durability data seems to be a serious block for the wide acceptance and application of FRPs in civil engineering, especially when the FRPs are exposed to one or combined conditions of water, alkaline solution, salt solution, static and dynamic forces, or extreme temperatures.[8–13]

Although lots of long-term durability studies have been conducted on FRPs used in aerospace, automotive, marine, and some industrial areas in the past several ten years, there is still a substantial lack of well-documented durability data for FRPs in civil engineering environments. This is partially due to the fact that the FRP materials used in civil engineering are quite different from those used in the other areas, in terms of the constituents of FRP composites and, sometimes, the manufacturing methods.[2] In addition, the environments faced in civil engineering also differ greatly from those in aerospace and the other application fields as mentioned. In view of this, a durability study of FRPs in various civil engineering environments is critical, as stated by the American Concrete Institute 440 committee.[14]

In cold regions, such as North America and north China, the influences of low temperature and freeze–thaw cycles on FRPs and FRP–concrete structures are of big concern[15–17] because microcracking of the resin matrix, debonding between the fiber and matrix, and the degradation of the adhesion of FRPs to the concrete substrates may occur. At subzero temperatures, the polymer matrix is reported to harden with an increased modulus; this results in enhanced mechanical properties of composites.[15,17,18] Dutta and Hui[17] studied two types of thick glass–FRPs (12.7–44.5 mm thick), which were subjected to a freeze–thaw cycle from −60 to 50°C,[17] and found that one commercially procured E-glass FRP indeed produced cracks after only 100 cycles. The other

Correspondence to: G. Xian (gjxian@hit.edu.cn and guijun.xian@gmail.com).

Contract grant sponsor: Program for New Century Excellent Talents in University; contract grant number: NCET-10-0065.

TABLE I
Properties of the Fiber Fabrics

Fiber fabric	Tensile strength (GPa)	Tensile modulus (GPa)	Elongation at break (%)	Density (g/cm^3)	Weight per square meter (g/m^2)
Carbon fiber	3.79	230	1.7	1.74	644
Glass fiber	3.24	72.4	4.5	2.55	915
Basalt fiber	3.30	105	2.6	2.65	380

plain-weave S-glass FRP showed a 6.2% decrease in Young's modulus and a 6.3% decrease in the shear modulus after 250 freeze cycles. As suspected,[17] the excursion to −60°C could easily push the matrix to its tensile strength (expected to be about 68.9–82.7 MPa), producing microscopic cracks, or a nonuniform curing across the thickness contributed to additional stresses in the center regions of these composites. Wu et al.[2] studied the freeze–thaw (4.4–17.8°C) effects on glass-fiber-reinforced polymer (GFRP) plates in the media of dry air, distilled water, and saltwater. As found, freeze–thaw cycles up to 1250 h and 625 cycles caused very insignificant effects on the flexural strength, storage modulus, and loss factor values of the FRP specimens in the adopted media. Karbhari[15] conducted a freeze–thaw test with the temperature ranging from −18 to 20°C on carbon-fiber-reinforced polymer (CFRP) and FRP wrapped concrete cylinders in a water bath. The CFRP plates showed an obvious decrease in the strength but an insignificant change in the modulus after 450 freeze–thaw cycles; this was attributed to the matrix cracking and debonding between the fiber and matrix.[15] The mechanisms were also advised by other researchers.[16] In addition, more attention was paid to the freeze–thaw resistances of FRP confined or strengthened structures.[19,20] Because those tests were only performed on FRP confined concrete structures, however, it was impossible to distinguish the freeze–thaw resistance of the FRPs.

Because the freeze–thaw resistance of FRPs has been considered as a serious concern for civil engineering applications in cold regions, in this study, we focused on the influence of freeze–thaw cycles on the tensile properties of GFRP, CFRP, and basalt-fiber-reinforced polymer (BFRP) epoxy wet layups. These FRPs have been frequently used for strengthening concrete structures. As is known, the thermal coefficient mismatching of the fiber and resin matrix may bring in debonding, microcracks, and even macrocracks of FRP plates.[15,17] Therefore, optic-fiber Bragg grating (FBG) sensors, which have been successfully applied in the strain monitoring of FRPs,[21] were embedded in the wet layups during sample preparation to monitor the strain evolution during the freeze–thaw cycles, with which the internal stress inside the FRPs could be evaluated to determine the possible degradation mechanisms. Tensile tests were conducted to illuminate the mechanical property degradation of the FRPs due to the freeze–thaw cycles.

EXPERIMENTAL

Materials

Epoxy resin (Tyfo S), kindly offered by Fyfe Co. (San Diego, California), was used as the resin matrix for the FRPs. The resin system consisted of a 4,40-isopropylidenephenol epichlorohydrin (similar to a diglycidyl ether of bisphenol A Epon 828 type system) combined with an aliphatic amine hardener in a 100 : 34.5 w/w ratio with a gel time of about 8 h at 23°C. The epoxy resin was indicated to be curable at ambient temperatures.

Both unidirectional carbon-fiber fabric (Tyfo SCH 41) and glass fiber fabric (Tyfo SEH 51A) were also kindly offered by Fyfe Co. The details of the fiber fabrics used in this work are given in Table I.

Sample preparation

Two layers of fiber fabrics with dimension of 250 × 250 mm^2 were cut and completely saturated with the epoxy resin with a wet layup process. To diminish the void content, a piece of poly(vinyl chloride) film was placed on the saturated fabrics, and a plastic trowel was used to squeeze the entrapped air and extra resin out. The sample was cured at ambient temperature for at least 7 days and then postcured in an oven at 60°C for 72 h. The resulting glass-transition temperature (T_g) of the composites was 82°C, which was measured with a differential scanning calorimeter (Linseis DSC PT10, Munich, Germany) at a heating rate of 10°C/min. The T_g of 82°C for the postcured samples could not be improved by further curing at high temperature (e.g., 110°C for 2 h) or a longer time at 60°C; this indicated that the epoxy system was fully cured with this postcuring process. This was also suggested by the datasheet of the resin system.

The fully cured wet layup plates were then cut into strips in the fiber direction with a diamond saw under water cooling. Figure 1 shows the photographs of the prepared FRP plates and cut strips.

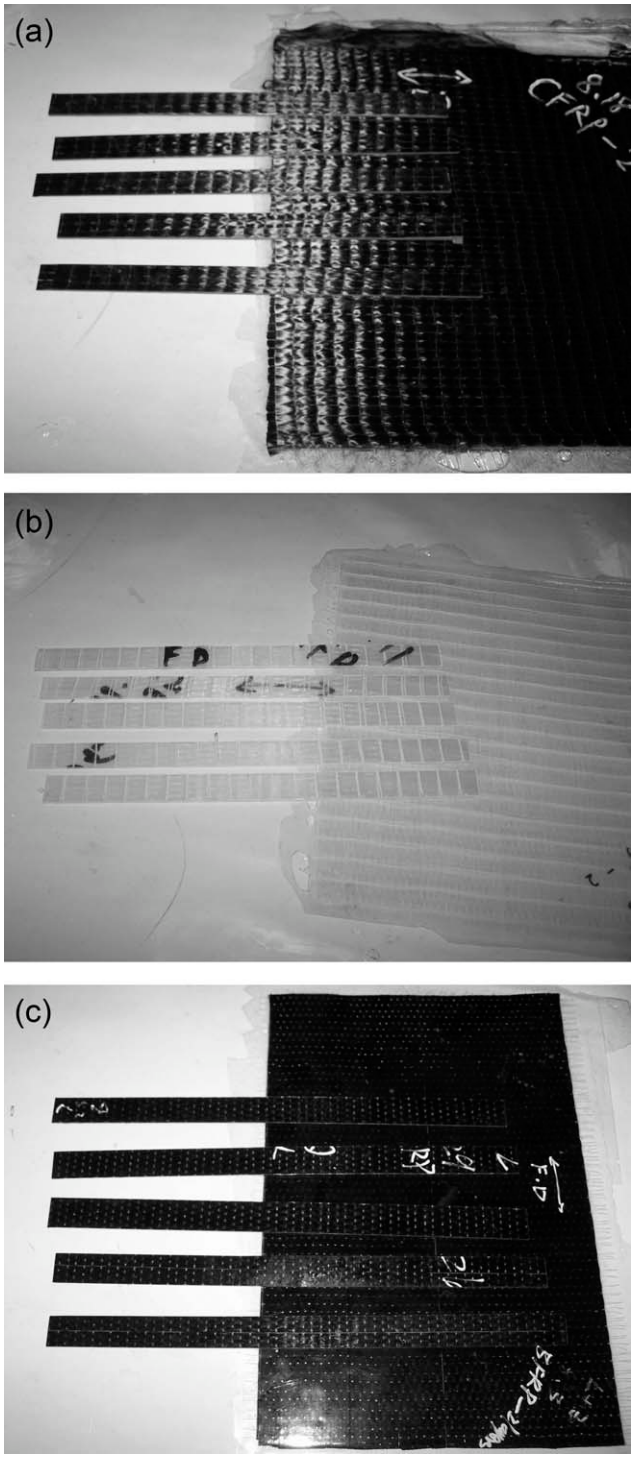

Figure 1 (a) CFRP, (b) GFRP, and (c) BFRP wet layup plates and cut strips for tensile testing.

To measure the internal stress during the freeze–thaw cycles, the FBG sensors were embedded in the interlayers of the FRP wet layups. The FBG sensors were carefully located in the fiber direction or perpendicular to the fibers. To facilitate comparison, a pure resin plate (4 mm in thickness) was also prepared with an embedded FBG sensor in the middle of the sample. The detailed procedure was discussed in our previous work.[22] The fabricated resin samples were cured with the same curing procedure for the FRP samples. In this work, the CFRP and BFRP samples were embedded with one FBG sensor in the fiber direction, and BFRPs were embedded with two FBG sensors, one along the fiber direction and one in the perpendicular direction.

Freeze–thaw resistance testing

The freeze–thaw cycle was realized with an oven and a freezer. One freeze–thaw cycle lasted 24 h and included a freezing state for 12 h and a thawing state for other 12 h. Samples were moved from the freezer to the oven or from the oven to the freezer after each 12-h period. The temperatures were set as −30°C in the freezer and 30°C in the oven. The average of the tested freezing temperatures was −27.3, and the thawing temperature was 32.7°C. The laboratory temperature, 12°C, was set as the equilibrium temperature, at which the internal strain was 0. Figure 2 shows the temperature variation with time. Note that the temperature of the oven was not stable, with several degree fluctuations because it was controlled by a thermocouple. In this work, 90 freeze–thaw cycles were performed.

Property characterization of the samples

The weights of the 25 × 25 mm^2 FRP plate samples were measured as a function of the number of freeze–thaw cycles. A test was done to track the weight changes of the samples.

The tensile properties of the unidirectional FRPs were tested according to ASTM D 3039 with a tensile speed of 2 mm/min. For each condition, five

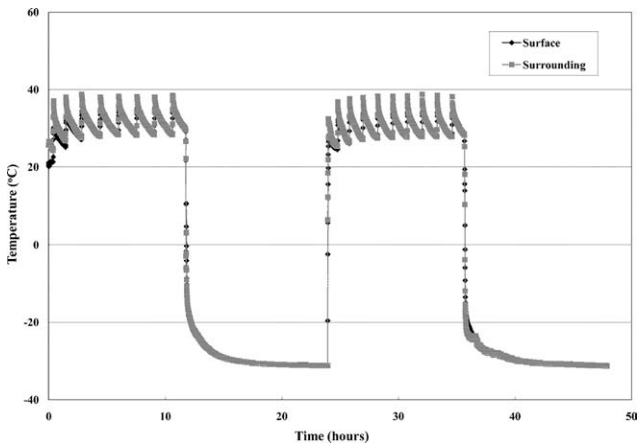

Figure 2 Evolution of the temperature with time during the freeze–thaw cycles. The temperature was measured with thermocouples attached to the FRP surface or the surroundings.

TABLE II
Tensile Properties of the Cured Two Layers of FRP Wet Layups Prepared in This Work and Tested According to ASTM D 3039 at a Tension Speed of 2 mm/min

FRP composite	Tensile strength (MPa)	Tensile modulus (GPa)	Elongation at break (%)
CFRP	971.4 ± 7.7	83.3 ± 7.7	1.12 ± 0.2
GFRP	517.9 ± 21.4	26.0 ± 3.8	2.04 ± 0.34
BFRP	602.9 ± 29.2	29.7 ± 2.8	2.2 ± 0.22

The fiber content was about 46.9 wt %.

samples were repeated, and the average results are reported. The tensile properties of the controlled samples are presented in Table II. Because the FRP samples were prepared with the wet layup procedure, the uniformity of the specimens was relatively low; this resulted in a high level of stand deviation.

The details of the internal strain tested with the FBG sensors can be found in our previous work.[22] It should be noted that we calibrated the reported strain in this work by changing the temperature.

RESULTS AND DISCUSSION

Weight change during the freeze–thaw cycles

As known, absorbed water is an important reason for the property deterioration for FRPs during the freezing process through volume expansion.[15] Therefore, the water uptake of the samples was first investigated in this study. The weight changes of the samples due to the freeze–thaw cycles are presented in Figure 3. As shown, all of the specimens showed decreases in weight. After 60 cycles, the weight reduction for both the CFRP and GFRP specimens was about 0.1%, whereas the BFRP sample showed a weight reduction of about 0.25%. Clearly, the weight reduction could be attributed to the drying effect during the thawing process. BFRP was first prepared and exposed to laboratory conditions for a longer time than the other two; this led to a little bit more moisture absorption. As expected, this was responsible for the higher weight loss of the BFRP specimens.

Because a very low content of moisture was absorbed by the FRP samples, the effect of water ingress on the resin microcracks and/or debonding of the fibers from resin could be avoided in this study.

Variation of the internal strain in the samples

The internal strain of the FRPs and pure resin plate was monitored as a function of the freeze–thaw times, which are shown in Figures 4–6. For one cycle, the samples were kept in the oven for 12 h and then moved to the freezer for another 12 h. When the samples were moved, the FBG sensor recorded abnormal high strain signals, as shown in the curves at the beginning of each cycle. Besides this, because of the instability of the oven temperature (as shown in Fig. 2), the measured strain showed the same fluctuation as the temperatures (Figs. 4–6). On the contrary, the strain of the specimens in the freezer was very stable.

Figure 4 presents the internal strain of the pure resin sample developed during the freeze–thaw cycles. As shown, when the temperature exceeded 12°C (which was room temperature, at which the internal strain was set as 0), a strain in expansion could be found. As the temperature decreased, a compression strain (shrinkage) was realized. The averaged expansion strain for four freeze–thaw cycles (Fig. 4) was 1890 με at 32°C (the average oven temperature), whereas the average shrinkage strain reached 2552 με at −27°C (the average freezer temperature).

In the fiber direction, for the BFRP plates, the expansion strain reached about 280.8 με in the oven,

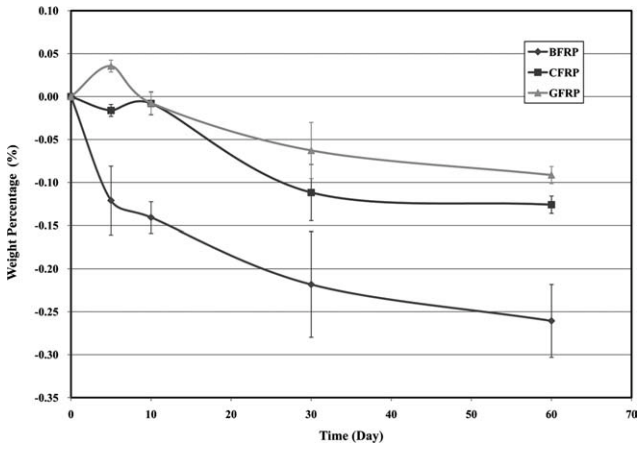

Figure 3 Weight changes of the FRP samples in 60 freeze–thaw cycles.

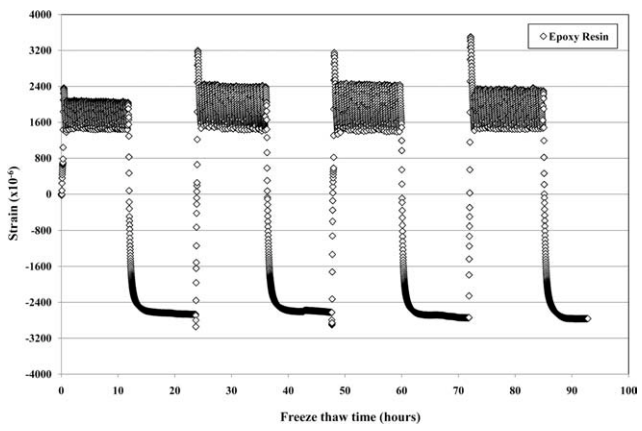

Figure 4 Evolution of the strain in the pure epoxy resin as a function of freeze–thaw.

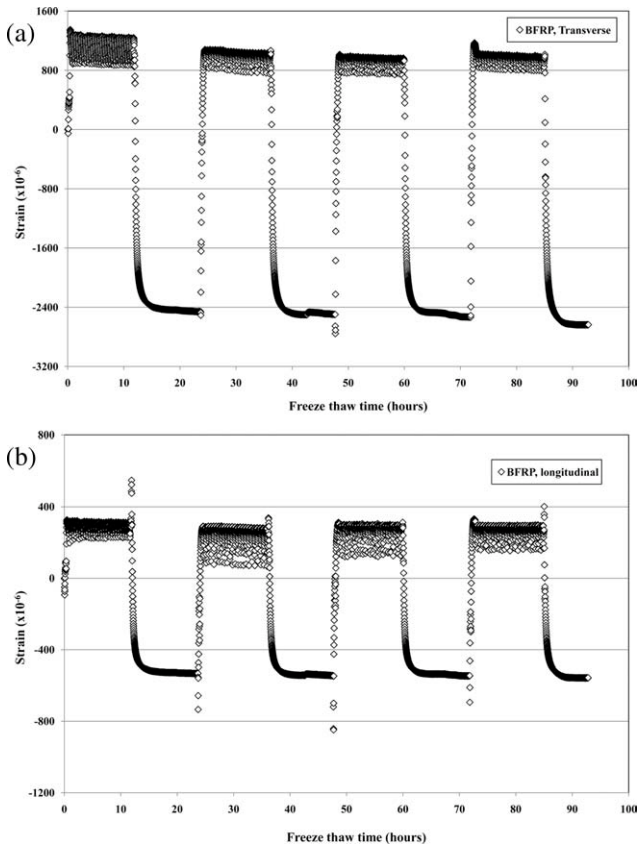

Figure 5 Evolution of the strain in the (a) fiber and (b) transverse directions of the BFRP plate as a function of freeze–thaw.

whereas the shrinkage strain reached 468.7 με in the freezer; these values were much lower than those of the pure resin (Fig. 4). Clearly, this could be attributed to the constraint effect of the basalt fibers in the longitudinal direction.[15,17] On the contrary, BFRP in the direction perpendicular to the fibers possessed an expansion strain of 989.5 με at the thaw temperature and a shrinkage strain of 2400 με at the freezing temperature. As seen, the strain values in the transverse direction were slightly lower than the strain of the pure resin. We interpreted this to mean that the expansion in the transverse direction was dominated by the resin, and the constraint effect of the fibers is much reduced.

Similarly, the strain changes due to the freeze–thaw cycles in the fiber direction for GFRP and CFRP were all much lower than that of the resin system (Fig. 6). For CFRP, the strain was 29 με in expansion and 84 με in shrinkage, whereas for GFRP, the strain was 247 με in expansion and 442 με in shrinkage. It should be noted that the CFRP sample showed the lowest strain change in the fiber direction, which could be assigned to the negative coefficient of thermal expansion (CTE) of the carbon fibers.[14] As reported, for T300 carbon fiber of Toray, CTE was -0.41×10^{-6} °C^{-1}.[23]

Table III summarizes the strain changes of the pure resin and three FRP plates. The internal strain measured by the FBG sensor as a function of the temperature is presented for each sample in Figure 7. Because the measured internal strain was caused by the thermal expansion of the composite system, the slope of the strain versus temperature could be used to estimate the CTE of the composite.[24] The estimated CTEs are listed in Table III. For the pure epoxy with a T_g of 82°C, the estimated CTE was 72.8×10^{-6} °C^{-1}. As is known, the CTE of an epoxy system depends on the chemical composition, conversion degree, and so on and may show a wide range from 10 to 100 $\times 10^{-6}$ °C^{-1}.[25–27] The CTE for this resin system was readily located in this range.

For GFRP and BFRP, the estimated CTE values in the fiber direction were very close, as shown in Table III. As presented in the datasheet of the used fibers, the glass fiber had a CTE of 5.4×10^{-6} °C^{-1},[28] whereas the basalt fiber had a CTE of 5.5×10^{-6} °C^{-1}. Besides the closed modulus of the glass and basalt fibers (see in Table I), it was not surprising for the CTE values of those FRP systems to be closed. Compared to GFRP and BFRP, CFRP showed a minimum CTE in the fiber direction, as mentioned

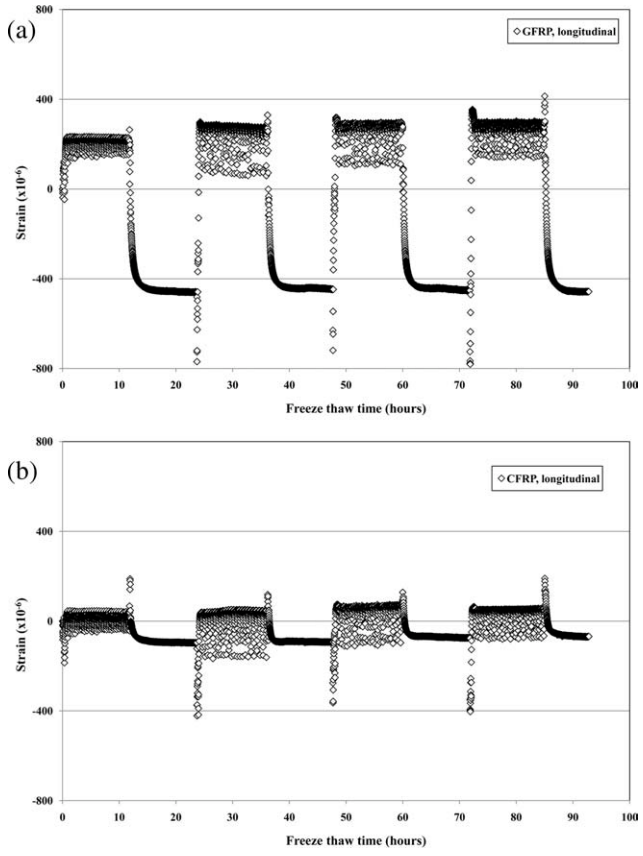

Figure 6 Evolution of the strain in the fiber direction of the (a) GFRP and (b) CFRP plates as a function of freeze–thaw.

TABLE III
Strains due to the Freeze–Thaw Cycle (−30 to 30°C) and Calculated CTEs for the Resin and FRP Wet Layup Plates

Sample	Expansion strain (10^{-6})	Shrinkage strain (10^{-6})	CTE ($\times 10^{-6}$ °C^{-1})[a]	CTE ($\times 10^{-6}$ °C^{-1})[b]
Epoxy resin	1890	2552	72.8	—
BFRP (longitudinal)	280.8	468.7	12.4s	7.73
BFRP (transverse)	989.5	2400	57.1	51.8
CFRP	29.0	84	1.9	0.72
GFRP	247.0	442	11.5	8.59

[a] Evaluated from the experimental results.
[b] Predicted with the Shapery model.

before, because of the negative CTE of the carbon fibers.

According to the Shapery model,[29] CTEs in the parallel (α_1) and transverse (α_2) directions of an unidirectional composite can be predicted with the following equations, respectively:

$$\alpha_1 = \frac{E_1^f \alpha_1^f V_f + E^m \alpha^m V_m}{E_1^f V_f + E^m V_m} \quad (1)$$

$$\alpha_2 = (1 + v^m)\alpha^m V_m + (1 + v_{12}^f)\alpha_1^f V_f - \alpha_1 v_{12} \quad (2)$$

where E_1 is the elastic modulus, V_f is the fiber volume fraction, V_m is the resin matrix fraction, v is Poisson's ratio, and v_{12} is the major Poisson's ratio of the unidirectional composites. The superscripts f and m denote the fiber and matrix, respectively. In this work, the fiber content was about 46.9 vol %, v_{12} of the fiber was set as 0.20, v_m was set as 0.3, and v_{12} was set at 0.3.[29] The predicted CTEs are presented in Table III. As shown, the predicted CTEs were all slightly smaller than the values determined experimentally. This could be understood by the fact that the samples were produced with the wet layup process and the fiber could not be uniformly distributed in the cross section. Therefore, the constraint effect of the fibers on the whole plate was diminished; this led to relatively higher CTEs of these FRPs.

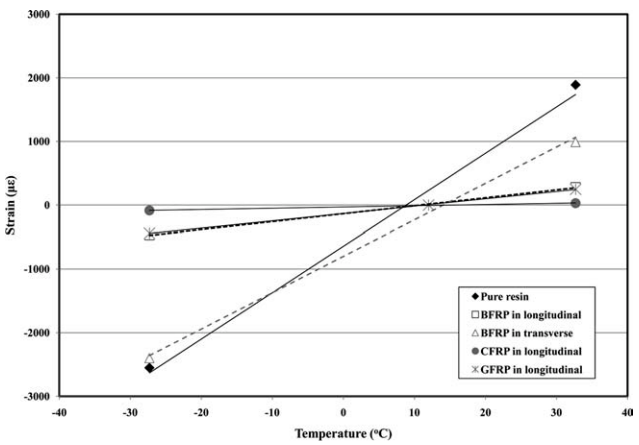

Figure 7 Linear fitting of the strain versus the freeze–thaw temperature for the estimation of CTE. The freezing temperature was tested as −27.3, the equilibrium temperature (strain = 0) was 12°C, and the thaw temperature was 32.7°C.

Because of the mismatching of the CTEs of the fiber and resin matrix, the stresses in the matrix around fibers could be developed during the freeze–thaw cycles. Hahn[30,31] proposed the following equation for the evaluation of the internal stress around fibers:

$$\sigma_m = (V_f E_f E_m)(\alpha_f - \alpha_m)(T - T_0)/(V_f E_f + V_m E_m) \quad (3)$$

where σ_m is the stress formed in the matrix in the longitudinal direction and T_0 is the stress-free temperature, taken as 12°C (the room temperature) in this work, T is the evaluation temperature. On the basis of the modulus of the pure resin (3.18 GPa), the internal stress formed during the freeze–thaw cycles could be determined and is presented in Table IV. As shown, the resin was subjected to a compression stress when the temperature was higher than 12°C and a stretch stress when the temperature decreased by −30°C.

For CFRPs, the stresses induced in the resin matrix around fibers were evaluated as 4.1 MPa in compression in the thawing state and 9.6 MPa in tension in the freezing state (Table IV). Those stress values were clearly higher than those of the BFRP and GFRP samples. As listed in Table IV, the compress stress reached 3.7 MPa, and the tension stress was 8.6–8.7 MPa for the GFRP and BFRP wet layups. For GFRP and BFRP, because of the closed CTEs and modulus, it was not surprising that the closed stresses developed in the matrix around the fibers.

It is worth noting that the ultimate strength of this epoxy system was 72 MPa; this was much higher than the internal stress developed due to the freeze–thaw cycles. The maximum internal stress of CFRP in tension was only about 13% of the ultimate strength of the resin. Therefore, it was almost impossible for the resin to experience microcracking due to the limited freeze–thaw cycles.

TABLE IV
Longitudinal Stresses in the Resin Matrix due to Freeze–Thaw

FRP composite	Stress (MPa)	
	Thaw state (30°C)	Freezing state (−30°C)
CFRP	−4.1	9.6
GFRP	−3.7	8.6
BFRP	−3.7	8.7

Note: a negative stress indicates compression stress.

Influence of the freeze–thaw cycles on the tensile properties of the FRPs

Figure 8 presents the variation of the tensile modulus, strength, and elongation at break of the BFRP, GFRP, and CFRP wet layups due to the freeze–thaw cycles. For both the BFRP and GFRP samples, after 90 freeze–thaw cycles, the changes of the tensile modulus and strength were located in the testing errors; this indicated a negligible effect of the freeze–thaw cycles. The elongation at break, however, increased with the freeze cycles. As indicated previously, the mismatching in the CTEs between the glass and basalt fibers and the epoxy resin may not have brought in a high internal stress (Table IV). Thus, the tensile properties were not adversely affected in the BFRP and GFRP samples. The result for GFRP was also supported by a literature study on GFRPs that were subjected to 625 freeze–thaw cycles from −17.8 to 4.4°C in dry air.[2] Because BFRP was just recently developed, at this time, no such freeze–thaw results have been reported.

Compared to the BFRP and GFRP samples, the CFRP wet layups showed a relatively more severe reduction in both the modulus and strength (Fig. 8). After 90 freeze–thaw cycles, the modulus was reduced by about 16% of its original level, and the strength reduction was about 18%. As reported, the high mismatching of CTEs between the fiber and matrix may bring in microcracks in the resin around the fibers and cause debonding of fibers from the matrix.[15,17] As shown in Table IV, however, due to the small internal stress formed in the matrix, the microcracking of the matrix in CFRP may not have occurred, despite the higher internal stresses compared to the cases of BFRP and GFRP. On the other hand, because of the intrinsic inertness of the carbon fiber, the interfacial adhesion between the fiber and resin was generally weak and may have been susceptible to internal stresses; this resulted in debonding of the carbon fiber and epoxy matrix. In view of this, the remarkable degradation of the tensile properties of CFRP may have been due to fiber debonding during the freeze–thaw cycles.

Karbhari[15] also reported a decrease in the tensile strength of water-saturated CFRPs subjected to 450 freeze–thaw cycles with the temperature ranging from −18 to 20°C. The tensile modulus of the CFRP was found to be unaffected by the freeze–thaw cycles.[15] This conflicted with our results; this difference may have been due to the differences in the temperature range, the resin matrices, and the curing conversion, fiber content, and degree of impregnation of fibers. As believed, such factors will readily affect the response of the CFRP samples to the freeze–thaw cycles. Dutta and Hui[17] also found that

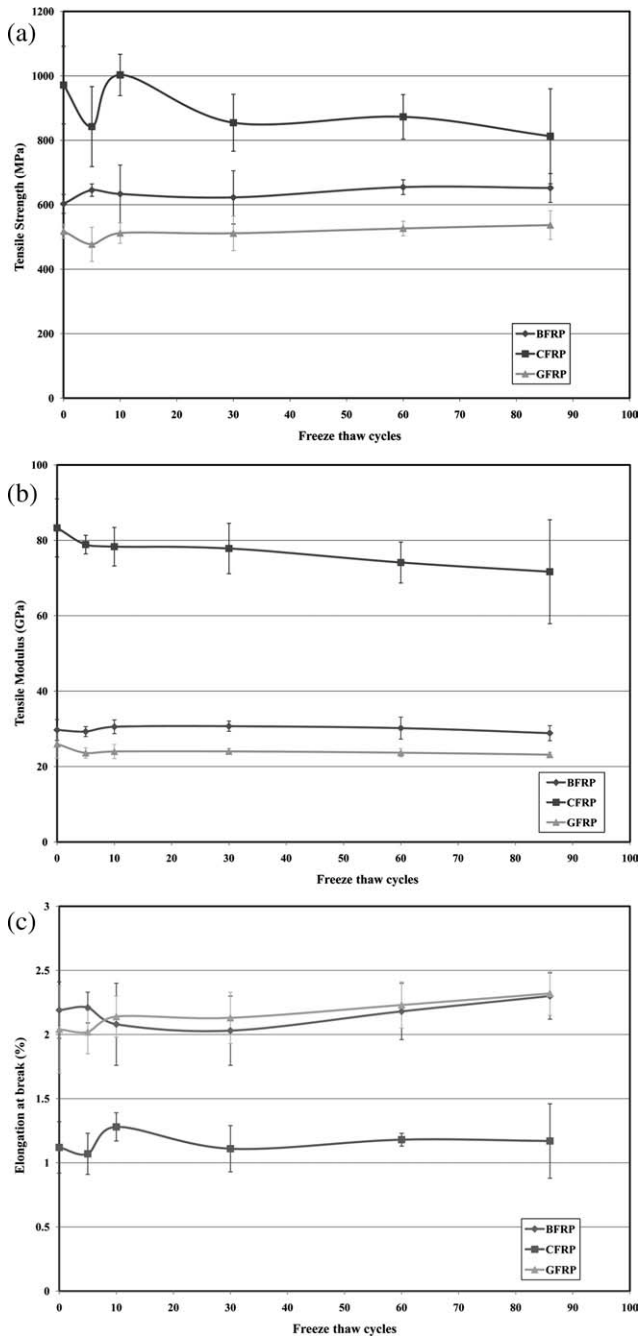

Figure 8 (a) Tensile strength, (b) modulus, and (c) elongation at break of the FRPs as function of the freeze–thaw cycles.

two GFRP samples with the same fiber type and manufacturing technology showed completely different freeze–thaw resistances.

CONCLUSIONS

In this study, the freeze–thaw resistances of unidirectional BFRP, GFRP, and CFRP wet layup plates were studied with temperature cycles ranging from −30 to 30°C. The strain evolution during the process was monitored with FBG sensors, which were embedded in the wet layup plates during sample preparation. The BFRP and GFRP wet layups showed closed CTEs ranging from 11.5–12.4 $\times$ 10^{-6} °C^{-1} in the fiber direction, whereas the CFRP plate showed a much lower CTE, about 1.9 $\times$ 10^{-6} °C^{-1} because of the negative CTE of the carbon fibers. In the transverse direction, the BFRP plate possessed a CTE of 57.1 $\times$ 10^{-6} °C^{-1}, a value slightly lower than that of the pure resin (72.8 $\times$ 10^{-6} °C^{-1}). The estimated CTEs of the FRPs were slightly smaller than the values predicted with the Shapery model because of the nonuniform fiber distribution.

The internal stress developed in the resin matrix during the freeze–thaw cycles in the fiber directions for FRPs was calculated with the estimated CTE values. In the CFRP wet layups, the tension stress was 9.6 MPa formed in the resin around the fibers in the freezing state, and the compression stress was 4.1 MPa in the thawing state; these values were slightly higher than those in BFRP and GFRP, which were 8.7 and 3.7 MPa, respectively. The internal stress formed during the freeze–thaw cycle was much lower than the ultimate strength of the pure resin; this indicated the impossibility of microcracking formed in the resin due to the limited freeze–thaw cycles.

The tensile properties of the BFRP and GFRP wet layups did not exhibit deterioration with the freeze–thaw cycles, whereas the CFRP wet layups showed decreases in the tensile strength of 16% and in the modulus of 18%. The deterioration of the tensile properties of the CFRPs was attributed to the possible debonding of the fiber and matrix due to the internal stresses formed during the freeze–thaw cycles.

References

1. Karbhari, V. M.; Chin, J. W.; Hunston, D.; Benmokrane, B.; Juska, T.; Morgan, R.; Lesko, J. J.; Sorathia, U.; Reynaud, D. J Compos Constr 2003, 7, 238.
2. Wu, H. C.; Fu, G.; Gibson, R. F.; Yan, A.; Warnemuende, K.; Anumandla, V. J Bridge Eng 2006, 11, 443.
3. Pendhari, S. S.; Kant, T.; Desai, Y. M. Struct Eng Mech 2006, 24, 1.
4. Pendhari, S. S.; Kant, T.; Desai, Y. M. Compos Struct 2008, 84, 114.
5. Rafi, M. M.; Nadjai, A.; Ali, F.; Talamona, D. Constr Build Mater 2008, 22, 277.
6. Mufti, A. A.; Bakht, B.; Banthia, N.; Benmokrane, B.; Desgagne, G.; Eden, R.; Erki, M. A.; Karbhari, V.; Kroman, J.; Lai, D.; Machida, A.; Neale, K.; Thadros, G.; Taljsten, B. Can J Civil Eng 2007, 34, 267.
7. Gheorghiu, C.; Labossiere, P.; Proulx, J. Compos A 2006, 37, 1111.
8. Yang, Q. A.; Xian, G. J.; Karbhari, V. M. J Appl Polym Sci 2008, 107, 2607.
9. Silva, M. A. G.; Biscaia, H. Compos Struct 2008, 85, 164.
10. Ouyang, Z. Y.; Wan, B. L. J Compos Constr 2008, 12, 425.
11. Ascione, F.; Berardi, V. P.; Feo, L.; Giordano, A. Compos B 2008, 39, 1147.
12. Karbhari, V. M. Int J Mater Product Technol 2007, 28, 217.
13. Chin, J. W.; Nguyen, T.; Aouadi, K. J Compos Technol Res 1997, 19, 205.
14. American Concrete Institute. ACI Committee 440 Report 440.2R-02; American Concrete Institute: Farmington Hills, MI, 2002.
15. Karbhari, V. M. J Compos Constr 2002, 6, 35.
16. Haramis, J.; Verghese, K. N. E.; Lesko, J. J. Annu Tech Conf - Soc Plast Eng 2000, 58, 3184.
17. Dutta, P. K.; Hui, D. Compos B 1996, 27, 371.
18. Karbhari, V. M.; Eckel, D. A. J Compos Technol Res 1995, 17, 99.
19. Green, M. F.; Bisby, L. A.; Beaudoin, Y.; Labossiere, P. Can J Civil Eng 2000, 27, 949.
20. Green, M. F.; Dent, A. J. S.; Bisby, L. A. Can J Civil Eng 2003, 30, 1081.
21. Zhou, G.; Sim, L. M. Opt Laser Eng 2009, 47, 1063.
22. Xian, G.; Wang, C.; Li, H. Proc SPIE-Int Soc Opt Eng 2010, 764909, 9.
23. Shindo, A. Comprehensive Compos Mater 2000, 2, 1.
24. Khonun, L.; Oliveira, R. D.; Michaud, V.; Hubert, P. Compos A 2011, 42, 274.
25. Yasmin, A.; Luo, J. J.; Abot, J. L.; Daniel, I. M. Compos Sci Technol 2006, 66, 2415.
26. Harsch, M.; Karger-Kocsis, J.; Herzog, F. J Appl Polym Sci 2008, 107, 719.
27. Karalekas, D.; Cugnoni, J.; Botsis, J. Compos A 2008, 39, 1118.
28. Dwight, D. W. In Comprehensive Composite Materials; Kelly, A., Zweben, C., Eds.; Elsevier: Amsterdam, 2000; Vol. 1.
29. Bowles, D. E.; Tompkins, S. S. J Compos Mater 1989, 23, 370.
30. Kim, K. S.; Hahn, H. T. Compos Sci Technol 1989, 36, 121.
31. Kim, K. S.; Hahn, H. T.; Croman, R. B. J Compos Technol Res 1989, 11, 47.